Università degli Studi di Napoli “Federico II”

Scuola Politecnica e delle Scienze di Base
Area Didattica di Scienze Matematiche Fisiche e Naturali

Dipartimento di Fisica “Ettore Pancini”

Laurea Magistrale in Fisica

Correlations in a stochastic model of neural networks

Relatori:
Prof. Antonio De Candia

Candidato:
Francesco Maria Schiavone
Matricola N94000470

A.A. 2019/2020

Contents

Introduction

The brain is a fascinating and complex machine presenting a wide range of features that modern computers are still far from reaching, as they are able to outperform it only in the matter of tasks based on arithmetic. This powerful instrument is composed of around 10^{11} neurons, cells arranged in networks and capable of rapidly propagating signals over large distances by generating electrical pulses, also known as spikes, that can travel along nerve fibers called dendrites. Such networks of cells connected with many others exhibit properties that cannot be inferred by simply studying the individual components, i.e. the single neurons, alone: this is the main characteristic of what are usually defined as *complex systems*, such as spin glasses, electrons in metals, polymers, climatic systems, etc. It is also for this reason that the study and the modelling of neural networks have benefited from the contributions of methodologies typical of statistical mechanics, ranging from the reformulation of McCulloch and Pitts model in terms of a spin magnetic system, passing through the introduction of an energy function by Hopefield and up to the employment by Amit et al. of the methods developed in the theory of spin glasses.

The following work aims to study, through the simulation of its time-evolution, the correlation functions of a neural network according to the number and the nature of the connections between its neurons. The model underlying this analysis is a stochastic version of the sigmoid rate model introduced by J. Cowan, also called the *stochastic rate model*, in which each neuron spikes with a probability per unit time dependent on its total synaptic input coming from the neurons connected to it, whereas the spiking activity decays in time at a constant rate.

This thesis is composed of three chapters and is organised as follows.

In the first chapter we discuss the neuron's structure and its main properties, focusing on the aspects that are most relevant to the modelling of neural networks. Subsequently, we describe how neurons communicate with each other and present the processes that make their interactions possible, namely the generation of action potentials. Moreover, we discuss another relevant aspect that affects neural activity: plasticity, responsible for learning, memory, and brain's ability to adapt.

In the second chapter we start by introducing one of the first significant models of neural networks: the model introduced by McCulloch and Pitts, which describes interactions between neurons using spin magnetic systems

as an example, in particular in terms of the Ising model. After this, we present the model used for our study, what we shall call the *stochastic rate model*, addressing its main characteristics and highlighting the aspects most relevant for our work focused on the study of time correlations. In this context, we shall also discuss the Gillespie algorithm, which we used to simulate the time evolution of our network.
Lastly, the third chapter is dedicated to the presentation of the numerical aspects for the main quantities characterising the model we recurred to in our work, and the simulations we have made with the aim to study, under a wide-sense stationarity hypothesis, how the number and the nature of the connections each nerve cell has in output affect the time-evolution of the network's activity in terms of a related autocorrelation coefficient.

Chapter 1

Neurons: physiology and properties

In the present chapter we focus on describing the general structure and the basic properties of the neuron, the cell representing the fundamental unit of neural networks, and on discussing how it works and communicates with other neurons.

A neuron, the elementary unit and main component of the nervous tissue in almost all animals, is an electrically excitable cell with the ability to communicate with other cells via electric pulses. The brain alone contains around 10^{11} of these cells [4]. Neurons can perform three possible functions, based on which we can make a first classification of their types: *sensory neurons* respond to external inputs such as light, temperature, and touch, thereby sending signals to the brain; this, in turn, communicates with *motor neurons* by sending them signals and enabling them to control aspects such as muscle contractions; lastly, the *connector neurons'* function is to connect neurons to other ones, specifically enabling connections between nerve cells in the central nervous system (consisting primarily of spinal cord and brain) and motor or sensory ones.
Neurons are mostly arranged in groups known as *neural networks*, which present several properties (very little power required to work, limited dimensions, high flexibility, efficient parallelisation etc.) that are highly desirable in artificial systems: this is also the reason behind the strong interest in neural computation.

1.1 Neuron Morphology

In biology there is no such a thing as a unique specimen of neuron, as there are different types of nerve cells inside the human brain and body [1]: what we will describe here is to be considered as an abstract neuron ("the" neuron) presenting the most generic and common characteristics shared by many of them that are regarded as the most relevant in their modelisation and artificial

implementation.
The neuron (see Figure 1.1) is a eucaryotic cell composed of three main parts: the cell body, also known as *soma*, the *dendrites*, and the *axon*.

The soma is the center of the cell and contains the nucleus, where the DNA is stored, the endoplasmatic reticulum, where the cell's proteins are synthesised, and several organelles, which perform specialised tasks.

From the soma extends a series of ramifying fibers called *dendrites*, which

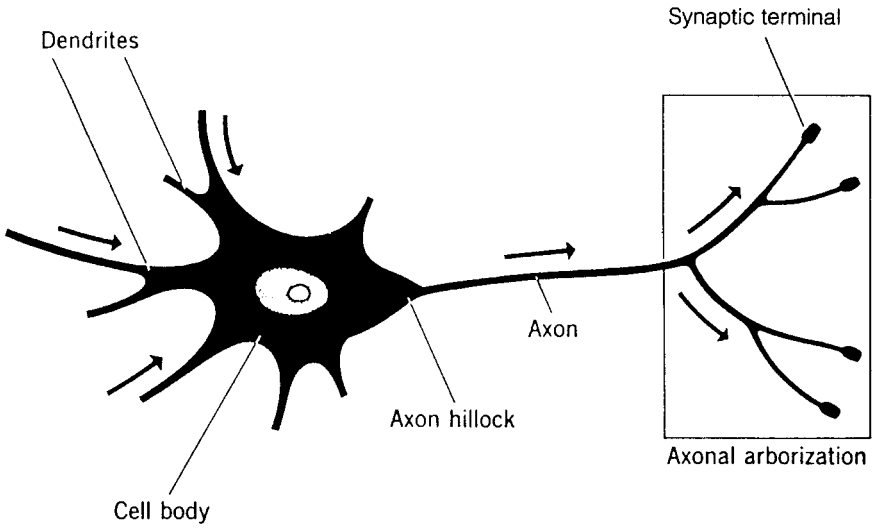

Figure 1.1: Here is an ideal neuron with all its main components discussed in this section. The arrows emphasise the unidirectionality of signal transmission in input and output, from one cell to another: the dendrites drive information inwards to the cell body, whereas the axon carries the signal (the action potential) outwards to other cells (not only neurons but also other kinds of cells, such as muscular ones) through synaptic terminals.
Figure adapted from [1].

are specialised in receiving chemical input-signals from other neurons in order to convert them into electrical ones to be sent to the cell body. Dendrites, together with the soma, constitute the input area of the neuron: their complex branching tree-structure allows each neuron to receive input signals from many other ones connected to it, usually leading to around $10^3 - 10^4$ connections per single nerve cell.

Similarly to the dendrites, another element protrudes away from the cell body, at a point of the soma called the *axon hillock*, namely the *axon*: it is a tubular structure whose function is to carry signals to other neurons and that can traverse large parts of the brain or even, in some particular cases, the whole body [3]. Near its end, the axon arborizes into branches that connect with other neurons, and the point at which two neurons communicate is called *synapse*; the cell transmitting the signal along the axon is also referred to as *presynaptic cell*, whereas the one receiving it in input is known as *postsynaptic cell*: such a distinction entails that there is a specific

directionality in the transmission of information from one neuron to the other, and goes under what is known as the *principle of dynamic polarisation* [2]. The presynaptic cell transmits signals from the end of its axon's branches, the *presynaptic terminals*, without having direct contact with the postsynaptic neuron: the two interacting elements, the terminal and what is typically a dendrite or the postsynaptic cell's soma, are actually separated by an empty space, the *synaptic cleft*.

The nerve cell is enclosed by a *neuronal membrane* which separates the intracellular plasma from the molecules and the interstitial fluid outside and, through the ion-channels that span on it, participates in controlling the flow of ions inwards and outwards, thereby regulating the neuron's electric potential and allowing response to stimuli and communication via signal transmission.

Ion channels are selective proteins that allow only one or a few types of cations and anions per each kind of channel to pass, predominantly potassium K^+, sodium Na^+, chloride Cl^- and calcium Ca^{2+}. Many channels are said to be *gated*, in other words they allow ions to flow across the membrane depending on external stimuli, with the kind of stimulus needed to change their state being different for each type: for example, *voltage-gated channels* are regulated by changes in voltage. On the other side, *resting channels* are non-gated channels that are normally open when the cell is at rest (i.e. it is not transmitting any signal) and are not influenced by extrinsic factors.

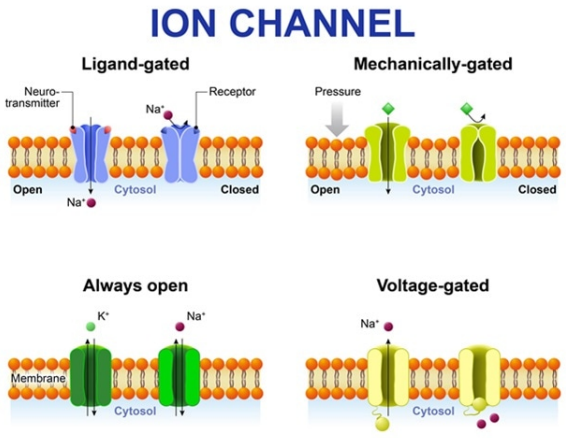

Figure 1.2: Examples of different gated ion channels, with their possible open and closed states, and a resting channel, which is always open; their function is to control the flow of ions across the membrane, thus regulating the neuronal potential and allowing the emission of signals from one neuron to others.
Figure adapted from `https://www.news-medical.net/health/Importance-of-Ion-Channels-in-the-Body-(Italian).aspx`.

1.2 Neural communication

Neurons communicate with each other via the generation and transmission of electrical pulses, namely *action potentials*, that travel down the axon of the presynaptic nerve cell and reach the input areas of the postsynaptic cells. Such signals in turn induce a change in the input-receiving neuron's potential and, if this potential varies above a common threshold, the signal can be transmitted further to other neurons.
In order to better understand neural communication, we must first discuss what affects the neuron's potential resting value and how it can change.

1.2.1 Membrane potential

All cells, neurons included, maintain at rest an electric potential difference between the intracellular fluid and the external medium, the *resting membrane potential* V_m; in the case of typical resting nerve cells this difference amounts to a value in a range between 60 and 100 millivolts [2,6], with the cell's interior being more negative than the exterior. By conventionally setting the external potential to zero, we say that the resting membrane potential is about $-65\ mV$ and the cell is polarised.

Such a gradient in the electric potential is reached and maintained thanks to the unequal distribution of ions on both sides of the membrane and to the permeability of the membrane to one in particular of those charged particles, the potassium cation K^+. The sodium-potassium pump, specifically, pumps sodium ions out of the cell and potassium back inside, in order to keep the concentration of the first species about ten times lower than on the outside and the one of the latter about twenty times higher [2]. Simultaneously, the elevate number of potassium-specific resting ion channels lets the K^+ cations leak out of the cell, according to the difference in the concentration gradient, at a rate higher than the rate at which sodium ions are allowed in, thus leading to a reduction of the inner positive charge, ergo to a minor potential if compared to the outside. In addition to this, inside the neuron there are also negative organic ions (A^-) that, since they are too large to diffuse across the membrane through the channels spanning its surface, cannot leave the cell and therefore contribute to its total negative potential.

Nernst and Goldman equations

As we have already stated, the diffusion of K^+, due to a chemical gradient, influences the electrical potential difference across the cell walls: higher potential outside the cell, lower inside; this difference tends to grow bigger as more and more potassium cations flow outside. Nevertheless, since they are positively charged, the increasing external potential tends to hinder their further flow through the ion channels; thus, ions are in general subject to two different kind of forces opposing each other: an electrical force, that depends on the potential difference (e.g. leading K^+ inside the cell), and a chemical

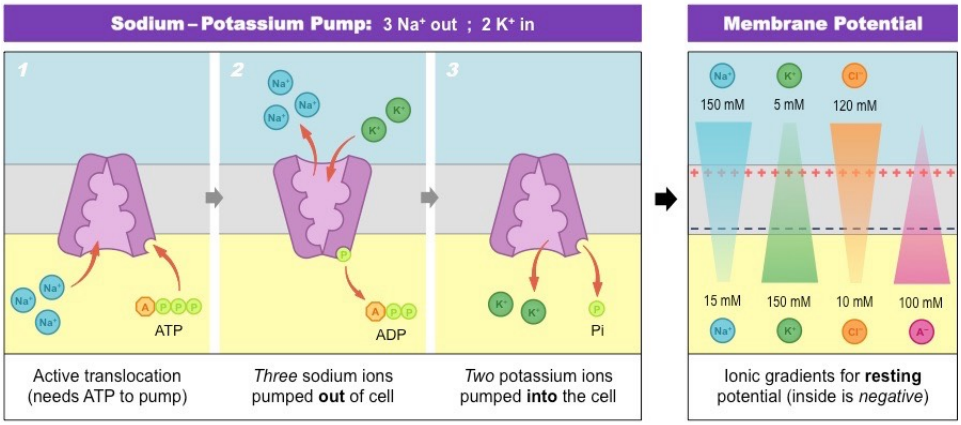

Figure 1.3: The sodium-potassium pump, on the left, is a transmembrane protein that helps to maintain the membrane potential constant in resting conditions. It expels 3 Na^+ for every 2 K^+ it leads in, consuming ATP in the process. This active pumping is in turn balanced by the passive flux of ions through membrane pores, the ion channels.
On the right are shown the typical chemical gradients for resting potential.
Figure adapted from `https://ib.bioninja.com.au/standard-level/topic-6-human-physiology/65-neurons-and-synapses/resting-potential.html`.

force, which on the other hand drives ions in order to compensate the concentration gradient across the membrane and, in the specific case of potassium ions, leads them outside the cell. At a certain point, the diffusion of ions across the soma walls makes the potential reach a value at which both forces balance each other: this is said to be the *equilibrium potential* V_{eq} of that particular species of ion.
The equilibrium potential for a generic ion, be it X, can be calculated through what is called the *Nernst equation* [2]:

$$V_{eq}^{(X)} = \frac{RT}{zF} \ln \frac{[X]_{out}}{[X]_{in}}$$

where, specifically,

- R is the universal gas constant, around $8.31\ J/molK$;
- T is the temperature expressed in kelvins;
- z is the valence of the ion X;
- F is the Faraday constant: $F = N_A \cdot e \simeq 9.65 \times 10^4\ C/mol$;
- $[X]_{out}$ and $[X]_{in}$ are the concentrations of the ion outside and inside the cell, respectively.

For example, for potassium cations (for which $z = 1$) across a membrane of a squid axon at room temperature ($25° \ C$, i.e. $298.15 \ K$), we have that $V_{eq}^{(K^+)} = -75 \ mV$ [2].

In order to determine the value of the resting membrane potential, however, one has to take into account the contribution of the main ions flowing across it, namely K^+, Na^+ and Cl^-: the potential is indeed not one only species equilibrium potential or a combination of all of them, as it is rather determined by their respective intra- and extracellular concentrations and also on how easily each chemical species can cross the membrane. This last aspect is taken into account via the introduction of the *permeability* P (expressed in units of velocity, cm/s), which resembles a diffusion constant and represents each ions' crossing rate. At this point, the membrane potential can be written as follows:

$$V_m = \frac{RT}{F} \ln \frac{P_K[K^+]_{out} + P_{Na}[Na^+]_{out} + P_{Cl}[Cl^-]_{in}}{P_K[K^+]_{in} + P_{Na}[Na^+]_{in} + P_{Cl}[Cl^-]_{out}}.$$

This is known as the *Goldman equation* and is only valid when the neuron is at rest and the potential is not changing [2]. In particular, when the permeability to one type of ion is higher than the permeability to the others, the former equation reduces to the Nernst equation for that specific ion species [2].

1.2.2 Action potential

The basis of neurons' signalling mechanism lies in their ability to alter quickly and significantly their membrane potential. The direct cause of such a change is of chemical nature: when an impulse reaches the presynaptic terminals, it activates voltage-gated ion channels, hence provoking an influx of Ca^{2+} that brings the vesicles present in the axon's ends to release neurotransmitters. These molecules cross the synaptic cleft and bind to the receptors on the synaptic membrane. At this point, the chemical action at the receptor sites, by activating gated channels, produces a change in the postsynaptic cell's membrane permeability to certain ion species, which results in a flux of ions inside or outside the cell that alters the membrane potential.

Depolarisation and hyperpolarisation: inhibitory and excitatory neurons

The activation of gated ion channels following the incoming of a signal can have two opposite effects on the membrane potential. If the net flow of ions is such that V_m increases towards the threshold limit (at $-55 \ mV$, [2]), the membrane is subject to *depolarisation*; since depolarisation enhances the neuron's ability to generate an action potential, such an effect is said to be *excitatory*. On the contrary, if the neurotransmitters induce V_m to grow more negative, ergo away from the threshold, the nerve cell incurs *hyperpolarisation*, which makes it less likely to transmit signals. Consequently, such an influence is defined as *inhibitory*.

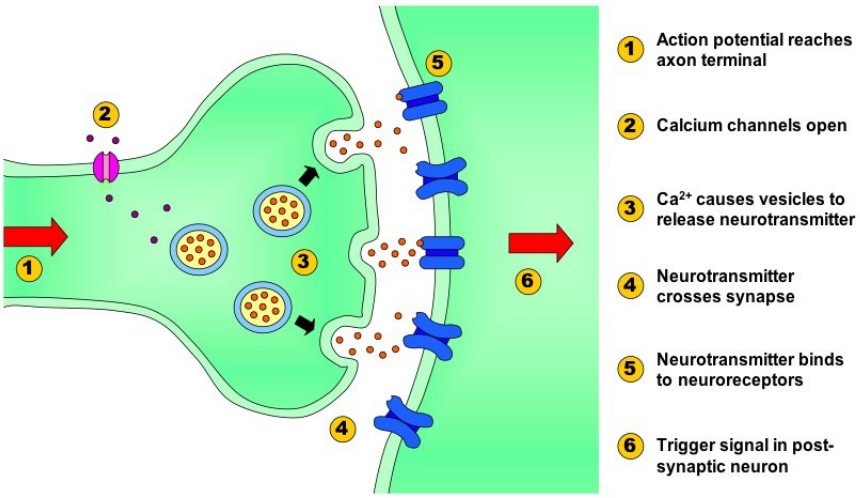

Figure 1.4: Representation of the steps constituting the process of chemical transfer across synapses.
Figure adapted from `http://www.old-ib.bioninja.com.au/standard-level/topic-6-human-health-and/65-nerves-hormones-and.html`.

Most neural models, as the ones presented in the next chapter, take into account the inhibitory and excitatory nature of interactions that occur among nerve cells by assuming that all synapses coming from a neuron have the same nature, being either all depolarising or all hyperpolarising [1]. It is hence logical, under such circumstances, to characterise neurons directly as either excitatory or inhibitory, depending on their influence on the statuses of the neurons they synapse upon.

Since a neuron receives electrical pulses from several neurons connected to it, two or more incoming signals combine their effects in the postsynaptic cell in what is known as *summation*; in particular, such a combination can lead to a reciprocal cancellation in case an inhibitory and an excitatory inputs cancel each other out. When spike-inducing stimuli arrive simultaneously from different presynaptic neurons, we say that the summation is *spatial*, whereas, in case they are generated in succession by a single presynaptic neuron and combine in the postsynaptic cell thereby letting the potential reach the threshold value, the summation is said to be *temporal*.

Generation of an action potential

If a neuron is depolarised sufficiently to have its membrane potential reach and even cross the threshold level, voltage-gated sodium channels start opening quickly: the following change in membrane permeability to such cations causes the inward flux of Na^+ to exceed the outward flow of K^+, hence resulting in a net influx of positive charges that induces an additional increase in depolarisation. This increment then causes even more

voltage-gated sodium channels to open, therefore bringing to more Na^+ crossing the membrane inwards and accelerating the depolarisation process even further. This avalanche progression produces then a pulse (the neuron is also said to be *firing*) with an amplitude of $100\ mV$ that lasts for about $1\ ms$ [3], the aforementioned *action potential* or *spike*, which travels down the axon (without changing its form, [5]) and reaches other cells.
The generation process of the action potential, the elementary unit of signal transmission, is *all-or-none*: this means that all stimuli below threshold will not produce any signal, whereas all stimuli above threshold will result in the same type of signal.
The form of the spikes does not carry any relevant information, as all the pulses of a neuron look alike: what rather matters is the number of pulses and the time intervals between them (with a chain of subsequent action potentials emitted by the same nerve cell being called a *spike train*). Furthermore, given the all-or-none nature of the signal generation, what really conveys information about the nature of the generating stimuli is the neural pathway along which the resulting signal travels [2].
While the potential peak is being reached, the variation of concentration gradients and membrane potential lets us assume a set of permeability ratios equal to $P_K : P_{Na} : P_{Cl} = 1.0 : 20 : 0.45$ [2] and, because of the dominance of the membrane permeability to sodium, the Goldman equation, as anticipated before, reduces the Nernst equation relative to Na^+:

$$V_m \simeq V_{eq}^{(Na^+)} = \frac{RT}{F} \ln \frac{[Na^+]_{out}}{[Na^+]_{in}} = 55\ mV.$$

Therefore at the peak of the action potential, when the membrane is the most permeable to sodium cations, V_m *approaches* $V_{eq}^{(Na^+)}$. Nevertheless, the non-absent permeability to K^+ and Cl^- results in respectively an influx of cations and an efflux of anions that oppose the further flow of sodium inside the soma, hence preventing V_m from actually reaching the equilibrium potential of sodium.

Once the peak has been reached at about $40\ mV$, two processes that end the action potential start coming into play: this phase is called *repolarisation*, which brings the membrane potential back to its resting value. Already during the spiking activity, sodium ion-channels begin to close, reducing the influx of Na^+; at the same time, the change in potential activates voltage-gated potassium channels, causing an increase in the K^+ flow outside the cell. These two processes combine to reduce the number of positive charges, thus inducing hyperpolarisation in the cell which brings it back to its resting membrane potential [2].

For a few milliseconds after firing, it is impossible for a neuron to start another pulse, since the equilibrium distribution of Na^+ and K^+ has to be re-established by the sodium-potassium pump: this time interval is called *absolute refractory period*; in addition, due to the hyperpolarisation process occurring after the spiking, for a longer period known as the *relative*

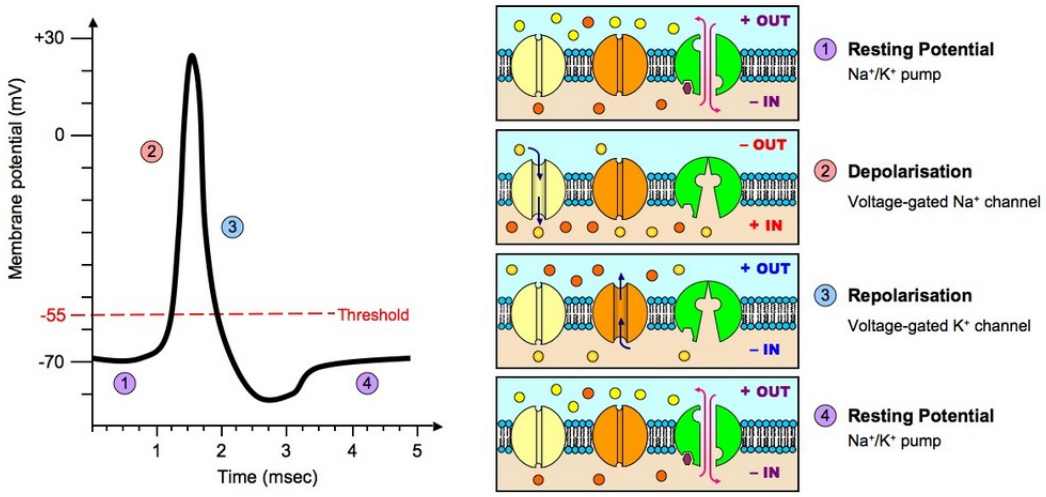

Figure 1.5: The graphic on the left shows the generation over time on the action potential, while explaining on the right its different phases in terms of the evolution of membrane permeability.
Figure adapted from `http://www.old-ib.bioninja.com.au/standard-level/topic-6-human-health-and/65-nerves-hormones-and.html`.

refractory period it is very unlikely for a neuron to fire again. The contribution of both these intervals characterises the neuron's *refractory period* [3].

1.2.3 Synaptic plasticity

The strength of synaptic transmission is not static, but can actually change over time: this neural feature is called *synaptic plasticity* and it consists in either the strengthening or the weakening over time of the synaptic interaction between neurons in order to enable the reshaping of the connections and, therefore, of the whole neural circuit. Plasticity is thought to be the mechanism underlying brain development, information storage and the ability to learn [3, 23].
There are several factors, of both presynaptic and postsynaptic nature, that can affect the intensity of the synaptic transmission between two nerve cells [23], thus contributing to the expression of plasticity:

- increase in the number of postsynaptic receptors;
- increase in receptors' response efficiency;
- increase in the neurotransmitter's concentration in the synaptic cleft either due to more releasing or less inactivation;
- increase in the number of synapses per cell;

- extension of the synaptic surface or reduction of the synaptic cleft's size.

In 1949 Donald Olding Hebb, trying to describe synaptic plasticity and how connections are modified, stated what is known as *Hebb rule* or *principle*, which postulates that if one neuron drives the spiking activity of another neuron it synapses upon, then the connection between them is potentiated [24]. Indeed, it has been observed that stimulating synapses through spike trains induces an increase in the synaptic strength that can last for periods ranging between tens of millisecond, in which case it is known as *short-term potentiation* (STP), to tens of minutes or longer, which is referred to as *long-term potentiation* (LTP) and is due to postsynaptic depolarisation, influx of Ca^{2+} and rise in the events of neurotransmitters release at presynaptic level [3, 5, 23]. Although excitatory and inhibitory synapses can exhibit plasticity, however, this has been generally less investigated for the latter [3], under both a theoretical and an experimental aspect, hence we shall refer strictly to the case of excitatory synaptic connections undergoing plasticity-related mechanisms.

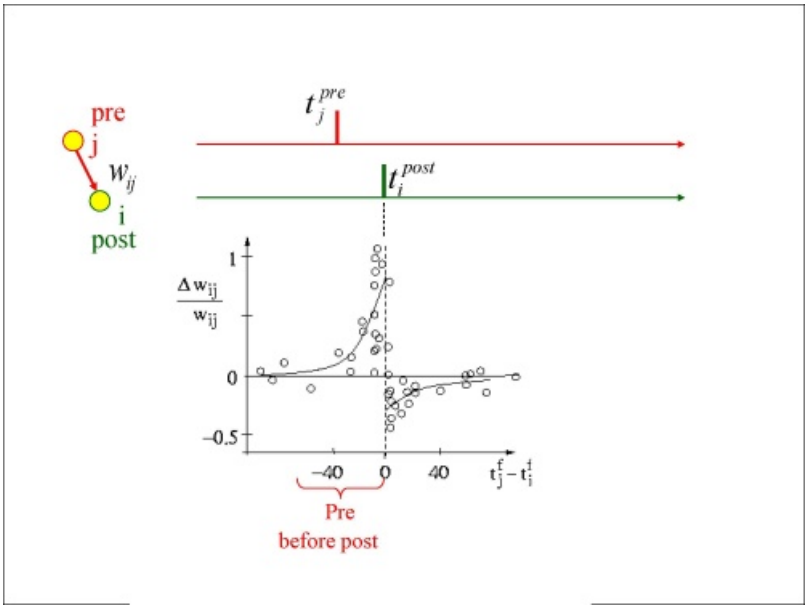

Figure 1.6: Spike-Time Dependent Plasticity (STDP). Here the change of the synaptic connections is shown as a function of the time-difference between pre- and postsynaptic spiking activities.
Figure adapted from `http://www.scholarpedia.org/article/Spike-timing_dependent_plasticity` (schematically redrawn after the results in [26]).

Hebb's original idea has been to this day extended to a general form in order to include another observed plasticity-related mechanism, namely the *long-term depression* (LTD) of the synaptic strength, which consists in the

weakening of the synaptic connection between the neurons that occurs when the input nerve cell fails to affect the other neuron's activity [3].
In agreement with Hebb's rule, it has been observed that changes in synaptic efficacy between the presynaptic neuron j and the postsynaptic cell i, Δw_{ij}, depend on the time difference $t_i - t_j$ between their respective spike times (*spike-time dependent plasticity*, STDP) [5, 25-27; see figure 1.6]. Specifically, the connection between them is strengthened ($\Delta w_{ij} > 0$) if the presynaptic spike occurs *shortly* before the postsynaptic neuron's spiking activity, whereas it is weakened ($\Delta w_{ij} < 0$) in case the sequence is reversed and the presynaptic neuron fires after the cell it synapses upon. In fact, if we look at such results in the light of Hebb's principle, this means that, in the first case, the presynaptic nerve cell takes part in the other cell's activity, while it does not in the other case, since the latter generates an action potential without the other driving it.

Chapter 2

Modelling neural networks

In the following chapter we show how several neural networks' features are included in their modelisation by first introducing McCulloch and Pitts model and then the *stochastic rate model*, the latter being the model underlying our whole analysis.

2.1 The McCulloch and Pitts model

When examined under a neurophysiological point of view, many models of neurons typically used for computational. problems and computer simulations are considerably simplified and "meagre"; however, as in many other modelling situations, many details regarding the single neuron may prove to be irrelevant in understanding the collective behaviour of systems of interconnected nerve cells.
In 1943 McCulloch and Pitts first proposed a simple mathematical model of a neuron [7] which still constitutes the basic reference in the field of neural modelling. They characterised the nerve cell as a binary threshold unit whose state can be either *firing* or *not firing*; such a state is affected by the inputs the neuron receives from those synapsing upon it in the following way: considering it to be the i-th neuron in a neural network, it can be either active or quiescent at time $t + \delta t$ according to

$$n_i(t + \delta t) = \theta \left(\sum_j w_{ij} n_j(t) - \mu_i \right), \tag{2.1}$$

where the sum runs over all the other j-neurons and $\theta(x)$ is Heaviside function

$$\theta(x) = \begin{cases} 1 & \text{if } x \geq 0, \\ 0 & \text{otherwise.} \end{cases}$$

Hence n_i can be either 1 or 0, which means respectively that the cell is firing an action potential or is depolarised. The weights w_{ij} represent the intensity of the synaptic interaction between neurons i and j and they are equal to

zero if the two are not connected. Moreover, their sign can be either positive or negative depending on the excitatory or inhibitory nature of the synapses involved. Lastly, μ_i represents the threshold potential for the i-th neuron: the cell starts firing only if the weighted sum $\sum_j w_{ij} n_j$ is bigger than or equal to this value: such a feature reproduces what we have previously described as the *all-or-none* aspect of neural spiking process.

This quite simple yet effective model therefore takes into account several

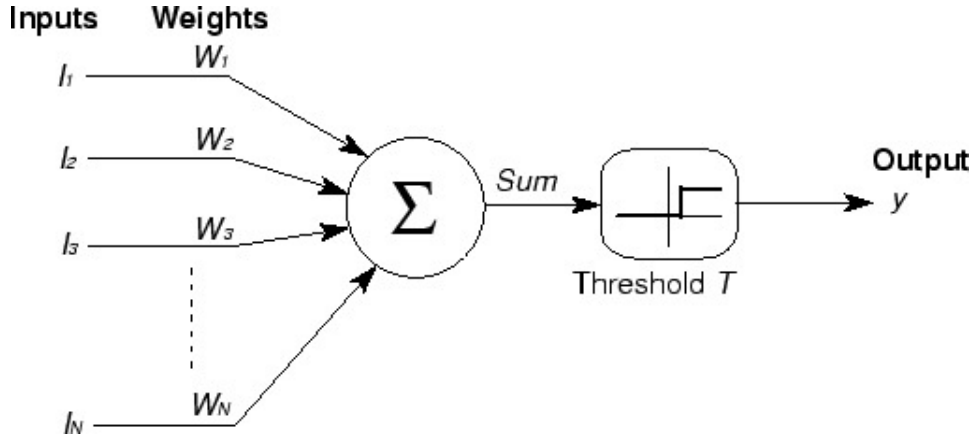

Figure 2.1: Graphical schematisation of McCulloch and Pitts model for a single unit (neuron), whose state (output y) is affected by the weighted summations of its input values, which is subsequently compared to a threshold value.
Figure adapted from `http://wwwold.ece.utep.edu/research/webfuzzy/docs/kk-thesis/kk-thesis-html/node12.html`.

of the neuronal properties described in the former chapter and also presents some of the main features of the stochastic rate model that is to be described in the next section. However, it is to be said that McCulloch and Pitts neuron fails to include some characteristics that can affect neural network dynamics [4]:

- the delay time δt is not the same for every cell, nor does the network evolution result from a synchronous update of the neurons' states;
- some neural cells can actually perform a nonlinear summation of weighted inputs and the resulting state can be described by a continuous number $n_i(t)$;
- the synaptic interaction strengths w_{ij} can vary over time due to neural plasticity;
- some features of neural interactions, such as the number of neurotransmitters released at the synaptic terminals, may change unpredictably, thus requiring the introduction of stochastic elements in the model.

Therefore, in order to include some of the aspects mentioned above into a mathematical model, a direct generalisation of McCulloch and Pitts model can be done by changing equation 2.1 as follows:

$$n_i(t + \delta t_i) = f\left(\sum_j w_{ij} n_j(t) - \mu_i\right),$$

where the state of activation $n_i(t)$ is now a continuous-valued number and the generic (not necessarily linear) function $f(x)$ is called the *activation function*.

Comparison with the Ising model and the energy function

McCulloch and Pitts neuron exhibits resemblance with the spin unit of the Ising model for a ferromagnet, as it also is a binary unit whose state s_i can be either $+1$ (*up*) or -1 (*down*); as a matter of fact, one can turn the McCulloch and Pitts unit state variable n_i into an Ising one s_i through a simple linear transformation

$$s_i = 2n_i - 1,$$

which leads to a different formulation of equation 2.1 in terms of the new variables:

$$s_i = \mathrm{sgn}\left(\sum_j w_{ij} s_j - \tilde{\mu}_i\right),$$

where $\tilde{\mu}_i = 2\mu_i - \sum_j w_{ij}$ in the new threshold value and

$$\mathrm{sgn}(x) = \begin{cases} 1 & \text{if } x \geq 0, \\ -1 & \text{otherwise.} \end{cases}$$

The analogy can be drawn further by considering that, taking an Ising magnet with no external magnetic field into account, the contributions from all other spins s_j influence s_i by generating a magnetic field

$$h_i = \sum_j J_{ij} s_j,$$

and the coefficients J_{ij} measure the strength of the interaction between s_i and s_j similarly as the coefficients w_{ij} do with synaptic strengths.
In 1982, in analogy with the Hamiltonian used in Statistical Mechanics, Hopefield introduced an *energy function* H into neural network theory [8], which, for a model based on the McCulloch and Pitts neuron, takes the following form:

$$H = -\frac{1}{2}\sum_j w_{ij} s_i s_j.$$

The matching is now complete: this function, resembling the equivalent Hamiltonian for an Ising magnetic system, always decreases as the network evolves according to its dynamical rules.

2.2 The stochastic rate model

The model underlying our whole analysis is a stochastic version of the sigmoid rate model introduced by J. Cowan in [9], called the *stochastic rate model* by the authors of [10], where they used it to study the formation of *neuronal avalanches*, observed *in vivo* and *in vitro* in several experiments, in networks composed of stochastic neurons that can be either excitatory or inhibitory. Neuronal avalanches are bursts of neural activity in which many neurons fire synchronously, preceded and followed by configurations that on the contrary are characterised by an absent firing activity [16]. The *size* of an avalanche is the total number of neurons activated during the burst.
The stochastic rate model is able to predict, when excitation and inhibition are closely balanced, the formation of avalanches whose size s follows a power-law distribution $s^{-\beta}$, also indicating that such a behaviour can be due to noisy network dynamics rather than a result of the network operating near criticality, across two different global ways of functioning [10]. The model is built as follows.
Each neuron can be in either an *active* (a) state, namely, it is firing or is going through its refractory period, or in a *quiescent* (q) one, meaning that it is at rest, being depolarised and able to turn active again; such states are designated in terms of a discrete variable $a(t)$ that can be equal to either one or zero, with the same interpretation as in the McCulloch and Pitts model for the variable $n(t)$. The nature of the connections each neuron has in output with other ones depends on its nature, which can be excitatory or inhibitory, and on the input-receiving neuron's type.

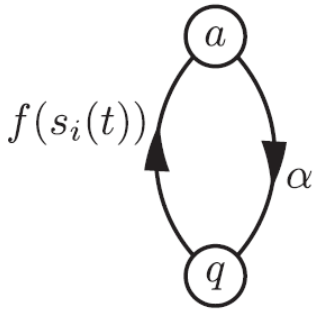

Figure 2.2: Representation of the state transitions ($a \to q$ and $q \to a$), with transition rates included, for a single neuron; in particular, $s_i(t) = \sum_j w_{ij} a_j(t) + h_i^{(ext)}$.
Figure adapted from [10].

What gives the model its name is that the transition of a neuron from one state to another has stochastic nature, with the state time evolution of a single neuron being a continuous-time, two-state Markov process. Specifically, the transition probability of the i-th neuron from active to quiescent in time dt is

$$\mathbb{P}(a \to q, \text{in time } dt) = \alpha dt;$$

when dt approaches 0, α stands for the decay rate of the active state of the unit. On the other hand, the transition probability from quiescent to active in time dt is generally different for each neuron, as it depends on how it interacts with the other nerve cells:

$$\mathbb{P}(q \to a, \text{in time } dt) = f(s_i(t))dt,$$

where

$$s_i(t) = \sum_j w_{ij} a_j(t) + h_i^{(ext)}$$

is the total synaptic input to the i-th neuron, resulting from the contribution of an external and constant input, $h_i^{(ext)}$, and a network input given by the sum over j above, whose weights w_{ij} are the strengths of the synaptic couplings (particularly, considering the unidirectionality of synaptic connections, w_{ij} represents the intensity of the connection that goes from j to i), and $w_{ii} = 0$ since a neuron does not interact with itself. Ergo, the firing rate is a function of the total synaptic input.
The function $f(s(t))$, called *response function*, is equal for every neuron and is chosen as follows:

$$f(s) = \begin{cases} \tanh(s) & \text{if } s > 0, \\ 0 & \text{if } s \leq 0. \end{cases}$$

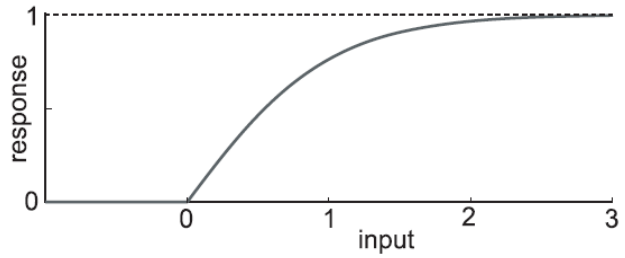

Figure 2.3: Plot of the response function versus the total synaptic input s. As it can be seen from the picture above, the choice made for the form of f leads to a neuron's firing rate to be equal to zero if s is below a threshold (zero, in the examined case), with growth close to linear as the synaptic input passes the threshold, until it saturates to a maximum value (i.e. one) when s grows bigger.
Figure adapted from [10].

As regards the aforementioned weights w_{ij}, their values depend only on the type of cells they connect, not on any other neural aspect: by introducing N_E and N_I, respectively the total number of excitatory and inhibitory neurons composing the network (the two satisfy, of course, the constraint $N_E + N_I = N$, where N is the total number of neurons), we have that the outgoing synaptic strength is set equal to

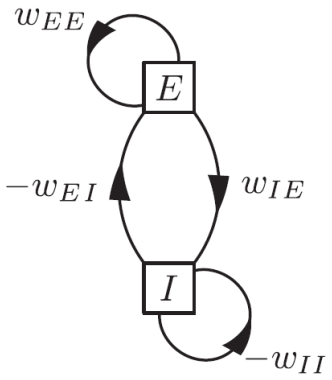

Figure 2.4: Representation of the synaptic strengths between the neurons of excitatory (E) and inhibitory (I) populations. The arrows indicate the direction of the input.
Figure adapted from [10].

- $\frac{w_{EE}}{N_E}$, if it goes from an excitatory unit to another excitatory one;
- $-\frac{w_{II}}{N_I}$, if it goes from an inhibitory unit to another inhibitory one;
- $\frac{w_{IE}}{N_E}$, if it goes from an excitatory unit to an inhibitory one;
- $-\frac{w_{EI}}{N_I}$, if it goes from an inhibitory unit to an excitatory one.

All the four coefficients, w_{EE}, w_{II}, w_{IE}, and w_{EI}, are positive. Such assumptions result in two populations of excitatory and inhibitory nerve cells interacting through different weights as in figure 2.4.

2.2.1 Network dynamics in the case of all-to-all connectivity

In case each neuron is connected to all the other neurons in the network, namely, when there is *all-to-all* connectivity, stochastic rate model network dynamics can be depicted as a random walk in a two-dimensional discrete states space, where each state is defined in terms of the k excitatory and l inhibitory *active* neurons, namely each state is a couple (k, l). Such a random walk goes from one state to another through one-step, single-component processes: this means that the total number of active units can either increase or decrease by one at a time. The effect is that the network state evolution can be represented as the system wandering on a lattice, as it is shown in figure 2.5 [10].
The system's stochastic evolution can be treated analytically by writing down the master equation relatively to the probability distribution $p_{k,l}(t)$, which indicates the probability that there are k excitatory and l inhibitory active neurons at time t, ergo the system is in the state (k, l). By looking at the central lattice point and the arrows in figure 2.5, we can see that we need to take 8 steps into account in order to express the time variation of the

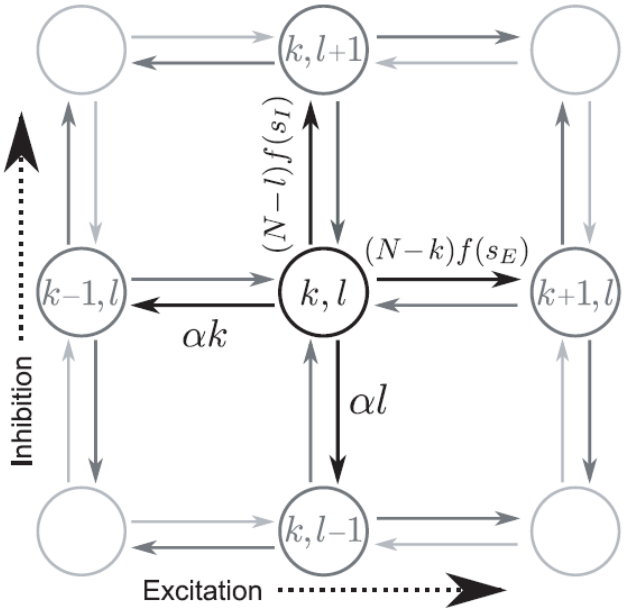

Figure 2.5: Random walk on a two-dimensional lattice representing the evolution of the network in terms of the number of active neurons belonging to the excitatory and inhibitory populations. Next to each arrow, which indicates the direction of the random walk single step, is the transition probability for that particular process.
Figure adapted from [10].

probability $p_{k,l}(t)$, with 4 of those steps giving a positive contribution and the other four a negative one.
Therefore, we shall now consider separately each of those 8 steps, according to the model's characteristics:

- from (k,l) to $(k-1,l)$: there are k active excitatory neurons, each turning quiescent at a rate equal to α, hence there is a flow of rate αk *out* of the state (k,l) proportional to $p_{k,l}(t)$, which means that the contribution to the time evolution of $p_{k,l}(t)$ is $-\alpha k p_{k,l}(t)$;

- from $(k+1,l)$ to (k,l): similarly to the former case, the $k+1$ excitatory neurons become quiescent at a rate α, thus leading the state towards (k,l) and resulting in a total positive contribution to the probability variation equal to $\alpha(k+1)p_{k+1,l}(t)$;

- from (k,l) to $(k,l-1)$: the situation is analogous to the one in the first case analysed, now with a negative term $-\alpha l p_{k,l}(t)$;

- from $(k,l+1)$ to (k,l): positive probability flow in the state (k,l) with a total contribution $\alpha(l+1)p_{k,l+1}(t)$;

- from (k,l) to $(k+1,l)$: there are $N_E - k$ quiescent excitatory neurons, each of them being ready to spike at a rate $f(s_E(k,l))$, yielding a term

$-(N_E - k)f(s_E(k,l))p_{k,l}(t)$, where

$$s_E(k,l) = \frac{w_{EE}}{N_E}k - \frac{w_{EI}}{N_I}l + h_E^{(ext)};$$

- from $(k-1,l)$ to (k,l): we have now a positive flow of rate given by $(N_E - k + 1)f(s_E(k-1,l))p_{k-1,l}(t)$;
- from (k,l) to $(k,l+1)$: the spiking of $N_I - l$ inhibitory neurons results in a rate term equal to $-(N_I - l)f(s_I(k,l))p_{k,l}(t)$, where the total input is now
$$s_I(k,l) = \frac{w_{IE}}{N_E}k - \frac{w_{II}}{N_I}l + h_I^{(ext)};$$
- from $(k,l-1)$ to (k,l): this last addend is similar to the one from $(k-1,l)$ to (k,l), as it is a positive rate flow caused by the activation of an inhibitory neuron, with a contribution equal to $(N_I - l + 1)f(s_I(k,l-1))p_{k,l-1}(t)$.

On the whole, all the deduced terms lead to the following master equation for the probability distribution $p_{k,l}(t)$:

$$\begin{aligned}\frac{dp_{k,l}}{dt}(t) = {} & \alpha[(k+1)p_{k+1,l}(t) + (l+1)p_{k,l+1}(t)] - \alpha(k+l)p_{k,l}(t) \\ & + (N_E - k + 1)f(s_E(k-1,l))p_{k-1,l}(t) \\ & + (N_I - l + 1)f(s_I(k,l-1))p_{k,l-1}(t) \\ & - [(N_E - k)f(s_E(k,l)) + (N_I - l)f(s_I(k,l))p_{k,l}(t)]p_{k,l}(t).\end{aligned}$$

2.2.2 The Gillespie simulation algorithm

Generally speaking, the method of evaluating the stochastic time evolution of a system is to derive and solve the relative master equation, which describes the time evolution of the probability distribution of the system's states through time, as we did in the former section by considering the case of all-to-all connectivity for a stochastic neural network. Nevertheless, although the master equation can be easy to write, solving it is a quite hard task; given this circumstance, despite being an exact and an elegant formulation of the stochastic evolution problem, it is not of much use. It is then useful to put the former approach aside and focus on how to simulate the stochastic time evolution of the neural network.
For this purpose, we resort to the *Gillespie algorithm*, an *event-driven* algorithm (in the sense that the simulation time advances only when the state of the network changes) first introduced by D.T. Gillespie in [12] in 1976 and originally intended to deal with the description of the time behaviour of a spatially homogeneous chemical system, whence the formalism we shall use to present it.
We firstly suppose that a volume V contains a mixture of X_i molecules of

chemical species S_i at thermal equilibrium, where $i = 1, \ldots, N$, and that these N species interact through M different chemical reaction channels R_μ, where $\mu = 1, \ldots, M$ [13]. The system state at time t is therefore determined by the n-uple $(X_1, \ldots, X_N)$, and we define h_μ as the number of distinct molecular combinations that react accordingly to the R_μ available in that state. Then we can introduce a total of M constants c_μ, which depend solely on the physical properties of the molecules and the system's temperature, such that the quantity $c_\mu dt$ represents the probability that a particular combination of molecules will react according to R_μ in the next infinitesimal time interval dt.
Starting from a given state $(X_1, \ldots, X_N)$ at time t, we need to know *when* the next reaction will occur and *which* of the M possible reactions it will be, so as to be able to tell how the system will evolve in time [12,13]. Because of the nature of the reactions, this is to be discussed in a probabilistic sense: we start by defining the probability distribution $P(\mu, \tau)$, that is the probability that, supposing to be in the state $(X_1, \ldots, X_N)$ at time t, the next reaction will be R_μ and will occur in a time interval equal to $[\tau, \tau + d\tau]$. In particular, $\tau \in [0, +\infty[$ and the joint probability density function $P(\mu, \tau)$ is called by Gillespie the *reaction probability density function* [13].
Hence, we are interested in determining the analytical expression for $P(\mu, \tau)$: this requires the definition of a_μ as

$$a_\mu dt = h_\mu c_\mu dt,$$

representing the probability that an R_μ reaction will occur in $[t, t + dt]$, when the state of the system is $(X_1, \ldots, X_N)$ at time t. The reaction density probability function can be then written as

$$P(\mu, \tau)d\tau = P_0(\tau)a_\mu d\tau,$$

where $P_0(\tau)$ is the probability that, in the state $(X_1, \ldots, X_N)$ at time t, no reaction will occur in the time interval $[t, t+\tau]$, whereas $a_\mu d\tau$ now represents the probability that an R_μ reaction will occur in $[t + \tau, t + \tau + d\tau]$. However, since $1 - \sum_\nu a_\nu d\tau'$ is the probability that no reaction will happen in a time period $d\tau'$ if we start from state $(X_1, \ldots, X_N)$ at time t [13], we have

$$P_0(\tau' + d\tau') = P_0(\tau') \left(1 - \sum_{\nu=1}^{M} a_\nu d\tau' \right),$$

from which we can derive the following form for $P_0(\tau')$:

$$P_0(\tau) = e^{-a_0 \tau},$$

where $a_0 \equiv \sum_{\nu=1}^{M} a_\nu$ is the total transition rate. Finally, we obtain the analytical form for $P(\mu, \tau)$:

$$P(\mu, \tau) = \begin{cases} a_\mu e^{-a_0 \tau} & \text{if } \tau \in [0, +\infty[\text{ and } \mu = 1, \ldots, M; \\ 0 & \text{otherwise,} \end{cases} \tag{2.2}$$

which is a joint probability density function on the space of the continuous variable τ and the discrete variable μ. Now, the simulation of the system's time evolution proceeds through the generation of couples (μ, τ) that follow the probability distribution whose form we have just obtained. In order to do so, we shall primarily write

$$P(\mu, \tau) = P_1(\tau)P_2(\mu|\tau), \tag{2.3}$$

where $P_2(\mu|\tau)$ is the conditional probability that the next reaction that will happen will be R_μ, given that it will occur at $t + \tau$. Because of the properties of joint probability density functions [22], we know that

$$P_1(\tau) = \sum_{\nu=1}^{M} P(\nu, \tau)$$

and, by substituting this into equation 2.3, we get that

$$P_2(\mu|\tau) = \frac{P(\mu, \tau)}{\sum_{\nu=1}^{M} P(\nu, \tau)},$$

which, if we go back to equation 2.2, leads finally to

$$P_1(\tau) = a_0 e^{-a_0\tau}, \quad 0 \leq \tau < \infty, \tag{2.4}$$

$$P_2(\mu|\tau) = \frac{a_\mu}{a_0}, \quad \mu = 1, \ldots, M. \tag{2.5}$$

It can be easily seen that both distributions are normalised.
Therefore, the Gillespie algorithm for simulating the stochastic time evolution of a chemically reacting system is composed of the following steps:

- the system is initialised by setting t to zero and choosing the initial values for the M reaction constants c_μ and the N numbers $X_1, \ldots, X_N$;
- the terms a_μ and their sum a_0 are calculated and stored;
- a couple (μ, τ) is generated according to the distributions in equations 2.5. Specifically, in order to generate those two numbers one can resort to using a random number generator of couples (u_1, u_2), where both u_1 and u_2 are extracted according to a uniform distribution on the interval $[0, 1]$: as a matter of fact, by making use of the *inversion generating method* (see Appendix), one can calculate τ as

  $$\tau = -\frac{1}{a_0} \ln(u_1)$$

  and μ as the number such that

  $$\sum_{\nu=1}^{\mu-1} a_\nu < u_2 a_0 \leq \sum_{\nu=1}^{\mu} a_\nu;$$

- time t is increased by τ and the populations X_i are modified according to the occurring of reaction R_μ;
- the new values of the rates a_μ are updated and so is a_0 afterwards.

The whole time evolution process is then obtained by repeating those steps until some predetermined halting condiction is verified, thus stopping the iterations.

Since we are dealing with neural networks modelled according to the stochastic rate model, we need to adapt the formalism above to our case. In particular, given a network of N excitatory and inhibitory neurons with generic connections, we have a total number of N "chemical species" S_i and the state of the system at time t is determined, once the connections among neurons are established, by $(X_1, \dots, X_N)$, where in our case X_i can be either 1 or 0 depending on whether the i-th neuron is active or quiescent respectively. Hence, for each neuron are available two mutually exclusive reactions:

$$\begin{aligned} active &\rightarrow quiescent \\ quiescent &\rightarrow active \end{aligned}$$

in which case the aforementioned rates a_μ are respectively

$$\begin{aligned} a_i^{(1)} &= X_i(t)\alpha; \\ a_i^{(2)} &= (1 - X_i(t))f(s_i(t)). \end{aligned}$$

Gillespie algorithm for all-to-all connectivity

If we consider a neural network with all-to-all connectivity, the number of variables X_i in the Gillespie algorithm reduces considerably. In fact, if we suppose to deal with N neurons, N_E of which are excitatory and N_I inhibitory, we can describe the system's state only in terms of the number of active excitatory and inhibitory neurons, k and l respectively, as we have already shown when deriving the system's master equation for this particular case.
Therefore, the number of X_i's shrinks to just 2 and we shall refer to them as k and l, whereas the total number of reactions becomes 4, namely

$$\begin{aligned} (k,l) &\rightarrow (k-1,l) \\ (k,l) &\rightarrow (k+1,l) \\ (k,l) &\rightarrow (k,l-1) \\ (k,l) &\rightarrow (k,l+1), \end{aligned}$$

with respective rates a_μ:

$$\begin{aligned} a_1 &= k\alpha; \\ a_2 &= (N_E - k)f(s_E); \\ a_3 &= l\alpha; \\ a_4 &= (N_I - l)f(s_I). \end{aligned}$$

Specifically, in our simulations, in the wake of what was done in [10], we choose that $w_E \equiv w_{IE} = w_{EE}$, $w_I \equiv w_{EI} = w_{II}$ and $h_i^{(ext)} \equiv h_0 \; \forall i$, thereby leading to $s_E = s_I \equiv s$, where

$$s(k,l) = \frac{w_E}{N_E}k - \frac{w_I}{N_I}l + h_0.$$

Chapter 3

Correlations analysis

In this last chapter we describe the main aim of our work, that is the study, by simulating the dynamic evolution of a neural network through the use of the Gillespie algorithm, of a specific type of time autocovariance function in dependence on how neurons are connected with each other. After discussing the premises and the principal quantities for our analysis, we present the results we have obtained and the conclusions we have come to.

3.1 Autocorrelation coefficient and connectivity index

Modern technologies such as multielectrode arrays have made it easier to measure correlations in neural networks and to understand their properties. Indeed, understanding how the brain works and how information is processed requires to study correlations between neurons [17]: for example, they can provide enlightening details about the architecture of neural networks, as with the connectivity in the retina and between nerve cells in cortex [17-19].
Dealing with a system of N interconnected nerve cells, N_E of which are excitatory and N_I inhibitory, we characterise its temporal evolution in terms of the total number of active neurons at time t and indicate it with $n(t)$, which can be regarded as an indicator of the network's activity. Specifically, in the hypothesis of *wide sense stationarity* [14] for the discrete stochastic process $\{n(t_1), n(t_2), \ldots, n(t_m)\}$, one of the two central quantities for us is a normalised version of autocovariance, that is the autocorrelation coefficient

$$\rho(t) = \frac{\langle n(t_i)n(t_i+t)\rangle - \overline{n}^2}{\sigma^2}, \tag{3.1}$$

where, since in general $\langle A\rangle$ is the average of A, $\overline{n} \equiv \langle n\rangle$ and $\sigma^2 = \langle (n-\overline{n})^2\rangle$, while t_i is a generic time. In fact, the stationarity of the time-evolution process lets us assert that the function above only depends on the time difference between two states $n(t_i)$ and $n(t_i+t)$ and that $\overline{n}$ and σ^2 are constant in time.

In particular, we have chosen t_i as t_{in}, namely the time such that $n(t_{in})$ is the initial state of the network at the beginning of each single time-evolution simulation process with the Gillespie algorithm.
We are then interested in studying the time evolution of $\rho(t)$ in dependence of the number of connections the units of the network can form with each other. Hence, another quantity of relevant interest is what we call the *neural network's connectivity index* γ: by indicating with N_O the number outgoing connections each cell has, we define it as

$$\gamma = \frac{N_O}{N}.$$

Moreover, once we have set a specific value for γ, we investigate and compare the functional forms of the related $\rho(t)$ for two different cases:

- **Case A**: each neuron can be connected only once with another unit, therefore N_O represents how many other units each cell is connected to;
- **Case B**: each neuron can establish more than one connection with the same j-th neuron, which then results in a stronger synaptic connection between the two. This in turn implies that the number of *different* other units each cell is linked to can be actually smaller than the expected value $N_O = \gamma N$, and that the synaptic strengths are not the same for every excitatory or inhibitory connection, which is what on the contrary happens in *case A* as we shall see from our choice for the w_{ij} in the next section.

3.1.1 Values for the stochastic rate model's parameters

We shall now discuss some of the simplifications we have made to approach our simulations and the values we have chosen for the parameters that characterise the stochastic rate model described in the former chapter.
For all our simulations, we worked with a neural network composed of $N = 1000$ units, with half excitatory and half inhibitory neurons.
As regards the deactivation rate, in the wake of paper [10] we have set

$$\alpha = 0.1\ ms^{-1},$$

that corresponds to a spiking state with a time constant $\alpha^{-1} = 10\ ms$: such a value takes the $1\ ms$ duration of the action potential into account, plus $9\ ms$ approximating the neuron's refractory period [10].
As for the activation rate, which depends on the total synaptic input

$$s_i(t) = \sum_j w_{ij} a_j(t) + h_i,$$

we have set $h_i \equiv h_0$ for all neurons, with $h_0 = 0.001$ in order to stimulate spontaneous network dynamics by choosing a weak external input.

Furthermore, the synaptic strengths w_{ij} are reduced to two different parameters: since w_{ij} represents the intensity of the connection *from* j *to* i, independently of i we have

- if unit j is excitatory, $w_{ij} = w_E/N_E$;
- if unit j is inhibitory, $w_{ij} = -w_I/N_I$;

where w_E and w_I are both positive, and $w_{ij} = 0$ if the two cells are not connected. We have chosen for both of them $w_E = w_I = 10$, in order to deal with a balanced network (i.e. inhibition balances excitation), since $w_- \equiv w_E - w_I \ll w_+ \equiv w_E + w_I$ as it has been done in [10]. The connections between units are generated randomly at the beginning of each run, without considering a significant geometrical structure of the network, and stay constant during the whole simulation. We have also introduced a constant $\beta = 1\ ms^{-1}$ which, similarly to α with the deactivation rate, sets a characteristic time

$$\beta^{-1} = 1\ ms$$

for the spiking rate. Specifically, the relation defining β is the following:

$$\mathbb{P}(q \to a, \text{in time } dt) = \beta f(s(t))dt.$$

Lastly, the values we have chosen for γ belong in a range between 0.005 (ergo 5 connections per neuron) and 1, where the latter sees each cell have 999 synaptic connections because of the absence of self-interaction. However, of the two aforementioned cases *A* and *B* of connections distributions types that we shall examine, only the first can be considered of all-to-all connectivity when $\gamma = 1$, as the second only entails that each unit has 999 links that, as we shall see, are very likely to be established multiple times between the same couples of neurons. Moreover, given the value of N we have chosen and the fact that the number of synapses per neuron in cortex is thought to be around $10^3 - 10^4$ [15], it seems reasonable to take the case of all-to-all connectivity into account.

The established values for the main quantities that characterise the stochastic rate model are displayed in the following table:

Parameter	N	N_E	$\alpha\ (ms^{-1})$	$\beta\ (ms^{-1})$	w_E	w_I	h_0
Value	1000	500	0.1	1	10	10	0.001

3.2 Simulation protocol and analysis of the autocorrelations

We have simulated around $50\ ms$ of our network's activity, collecting information relevant to the reconstruction of $\rho(t)$ in a linear way every $1\ ms$ and starting from $t = 0$, which therefore leads to 51 temporal points for the

time-evolution evaluation of the autocorrelation coefficient. Between each of the time steps, the system has been made evolve according to the Gillespie algorithm. This time evolution process has been repeated in its entirety in several iterations per each simulation: once arrived at the last time step, the network's last state was used as the initial state of next iteration (the aforementioned $n(t_{in})$). For each of the values we have considered for γ, we have run a total of 100 simulations and calculated $\rho(t_i)$, for $i = 0, \ldots, 50$, by averaging on all the 100 estimations obtained for it.
The starting state of every network had every unit in the quiescent state and the first iterations of every simulation have been discarded and not included in the calculation of the correlations, as they have been regarded as a thermalisation phase.
The two semilogarithmic plots in figures 3.1 and 3.2 show the various reconstructed $\rho(t)$'s, depending on different choices for the value of the connectivity index, in the two cases we have defined as *case A* and *case B*.
As it can be visually noticed by looking at the two groups of plots, for each value of γ the resulting $\rho(t)$ decreases monotonously towards zero as t grows: the state of spiking activity of the system is less and less dependent on the initial state as the network evolves. Moreover, we can see that the outcomes are not the same in the two different cases *A* and *B* and we observe no specific trend for the time evolution of $\rho(t)$ by varying the parameter gamma γ.

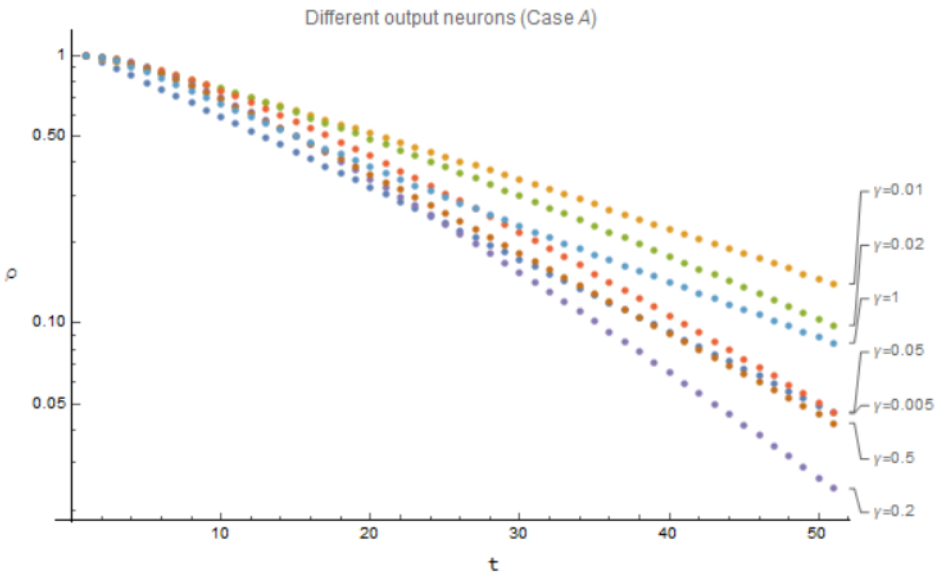

Figure 3.1: **Case A**: semilogarithmic plot of the time evolution of $\rho(t)$ for $\gamma \in \{0.005, 0.01, 0.02, 0.05, 0.2, 0.5, 1\}$, when each neuron can only be connected to the same neuron once. The time-scale on the *x-axis* is in milliseconds.

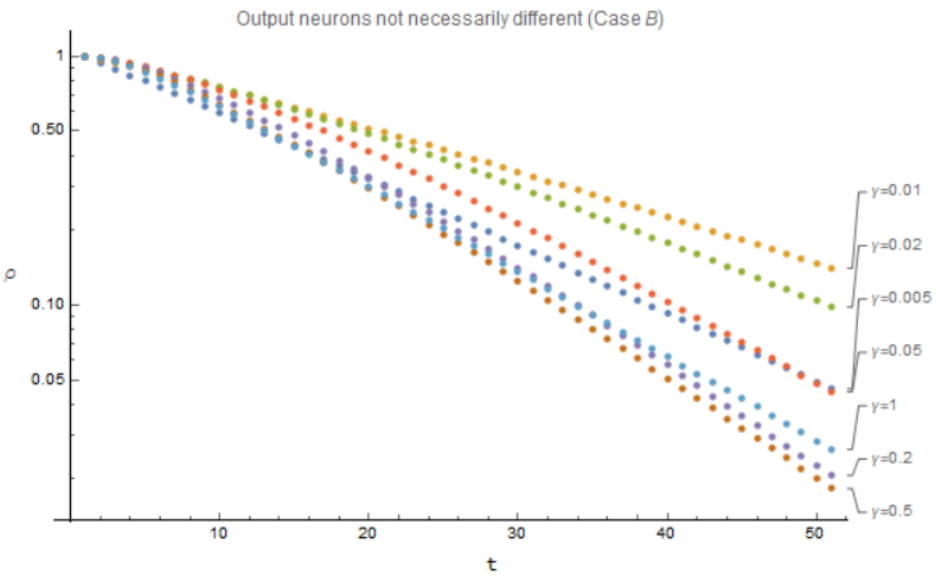

Figure 3.2: **Case B**: semilogarithmic plot of the time evolution of $\rho(t)$ for $\gamma \in \{0.005, 0.01, 0.02, 0.05, 0.2, 0.5, 1\}$, when each neuron can establish more than one connection with the same neuron. The time-scale on the *x-axis* is in milliseconds.

For the sake of clarity and in order to better highlight the differences between the results that out simulations have yielded, we compare now the plots for $\rho(t)$ considering each of the values for the parameter γ singularly in figures from 3.3 to 3.9.

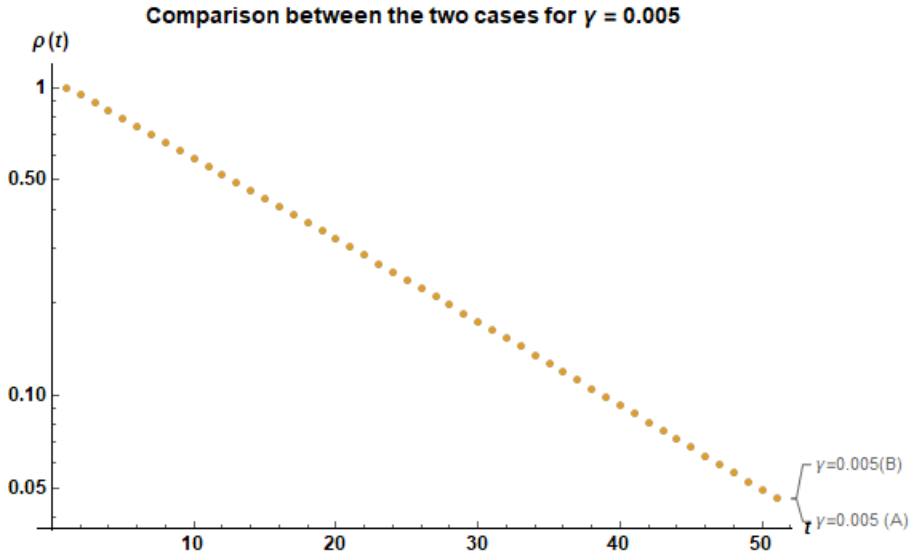

Figure 3.3: Comparison of the semilogarithmic plots of $\rho(t)$ in the two cases for $\gamma = 0.005$. The time-scale on the *x-axis* is in milliseconds.

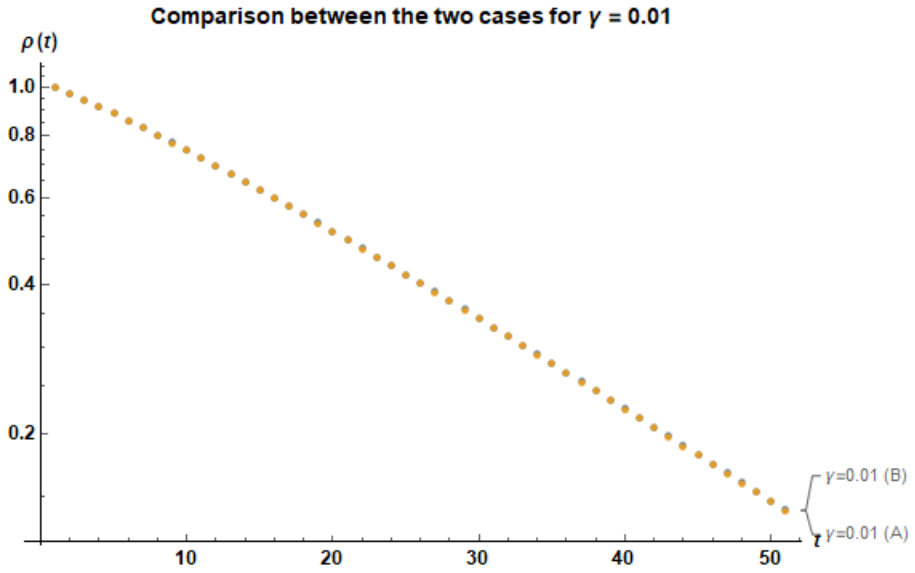

Figure 3.4: Comparison of the semilogarithmic plots of $\rho(t)$ in the two cases for $\gamma = 0.01$. The time-scale on the *x-axis* is in milliseconds.

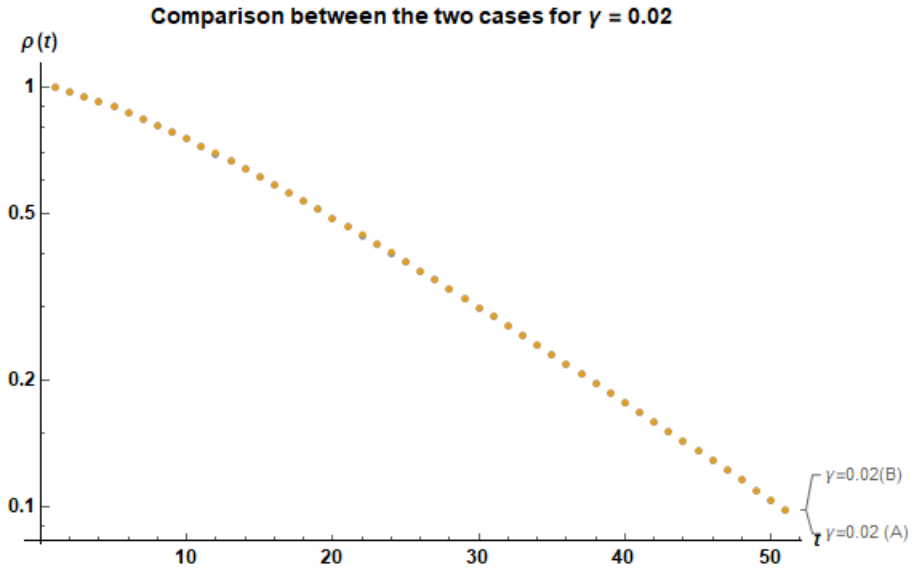

Figure 3.5: Comparison of the semilogarithmic plots of $\rho(t)$ in the two cases for $\gamma = 0.02$. The time-scale on the *x-axis* is in milliseconds.

3.2.1 First results and decorrelation time

Now we discuss the first results we have come to through the analysis of the time evolution of the various ρ's. By looking at figures 3.3-3.9, the difference between the time evolution of $\rho(t)$ in cases *A* and *B* becomes more evident as γ grows bigger: as a matter of fact one could expect the chance that between two neurons more than one connection is established to increase as the number of connections each nerve cells can form goes from just 5 to 999, each of them being generated randomly and independently.

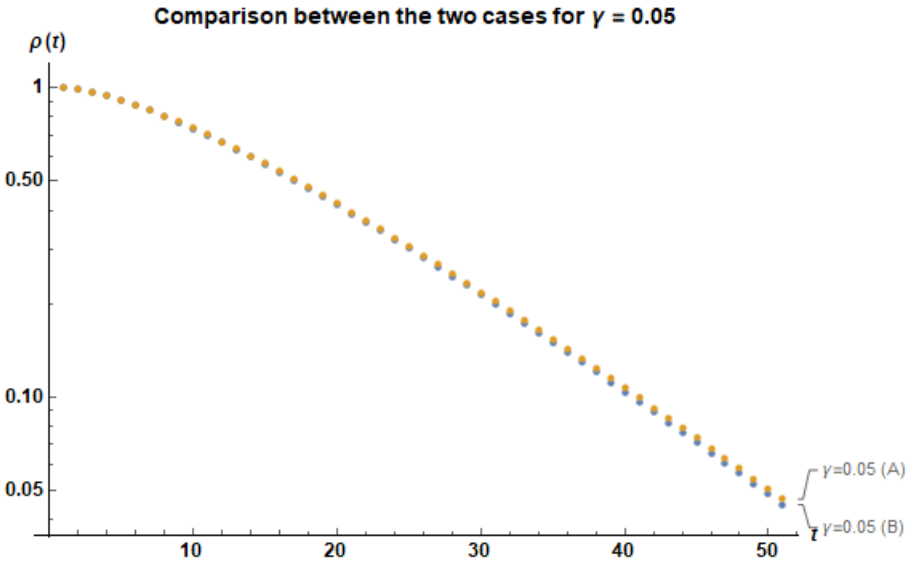

Figure 3.6: Comparison of the semilogarithmic plots of $\rho(t)$ in the two cases for $\gamma = 0.05$. The time-scale on the *x-axis* is in milliseconds.

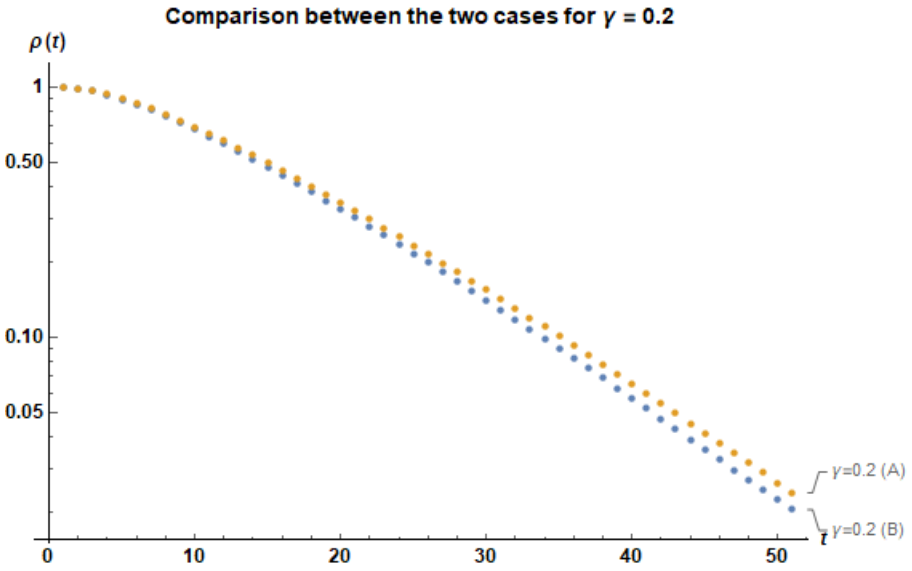

Figure 3.7: Comparison of the semilogarithmic plots of $\rho(t)$ in the two cases for $\gamma = 0.2$. Starting from this value of γ the difference between the time evolutions of the two $\rho(t)$ becomes more evident, resulting in a faster-decreasing trend in *Case B*. The time-scale on the *x-axis* is in milliseconds.

Therefore, under the premises characterising *case B*, the bigger γ is, the bigger is the chance that each unit actually forms more than one connection with the same neuron, which means that the number of different units each neuron synapses upon tends to be smaller than the value γN. Moreover, unlike *case A*, the synaptic strengths do not have the same value for all excitatory and inhibitory connections: this must play a role in ρ's time

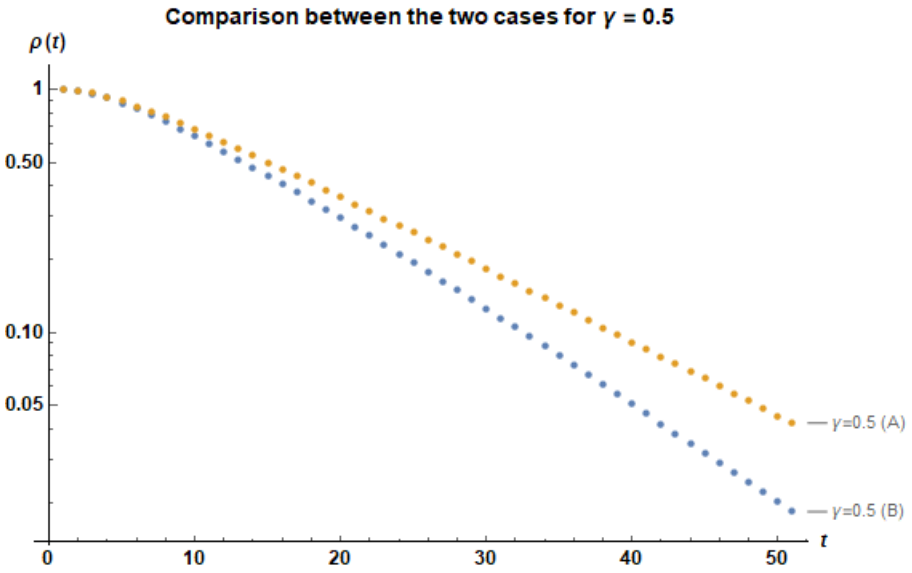

Figure 3.8: Comparison of the semilogarithmic plots of $\rho(t)$ in the two cases for $\gamma = 0.5$. The time-scale on the *x-axis* is in milliseconds.

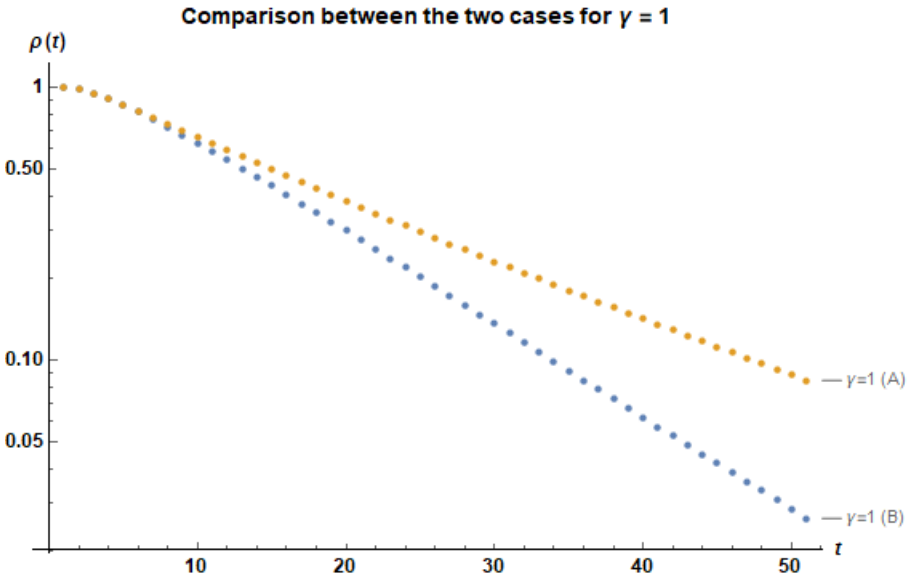

Figure 3.9: Comparison of the semilogarithmic plots of $\rho(t)$ in the two cases for $\gamma = 1$. Here the difference between the two cases is the most evident. The time-scale on the *x-axis* is in milliseconds.

evolution since the difference in trends appears to follow a precise pattern, whereas it does not if we base it solely on a different effective value of γ, as seen from figures 3.1 and 3.2.
Hence, the first qualitative information we can deduce is that the evolution of the autocorrelation function depends on both the connectivity (although $\rho(t)$ does not appear to change according to a specific trend as γ varies), more generally considered as the number of connections each neuron has in

output, and the connection strengths; specifically, we see that it decreases faster and gets closer to zero when neurons have the chance to form stronger connections with some of the other neurons.

Decorrelation time

In order to carry out a more quantitative analysis of the results we have obtained, we introduce the *decorrelation time* τ_γ, defined as the time such that

$$\rho(\tau_\gamma) = \frac{1}{e} \simeq 0.368, \tag{3.2}$$

for each of the autocorrelations related to a specific γ.
Given the discrete points we have for the time evolution of $\rho(t)$, we have extracted τ_γ by first identifying two consecutive time-step points t_a and t_b such that $\rho(t_b) \leq 1/e \leq \rho(t_a)$ with $t_a < t_b$, and then by approximating the analytic form of $\rho(t)$ for $t \in [t_a, t_b]$ through a linear interpolation:

$$\rho(t) = \frac{\rho_b - \rho_a}{t_b - t_a}(t - t_a) + \rho_a,$$

where $\rho_a \equiv \rho(t_a)$ and $\rho_b \equiv \rho(t_b)$. At this point τ_γ has been estimated by solving equation 3.2, which is straightforward, leading to

$$\tau_\gamma = \frac{t_b - t_a}{\rho_a - \rho_b}\left(\rho_a - \frac{1}{e}\right) + t_a.$$

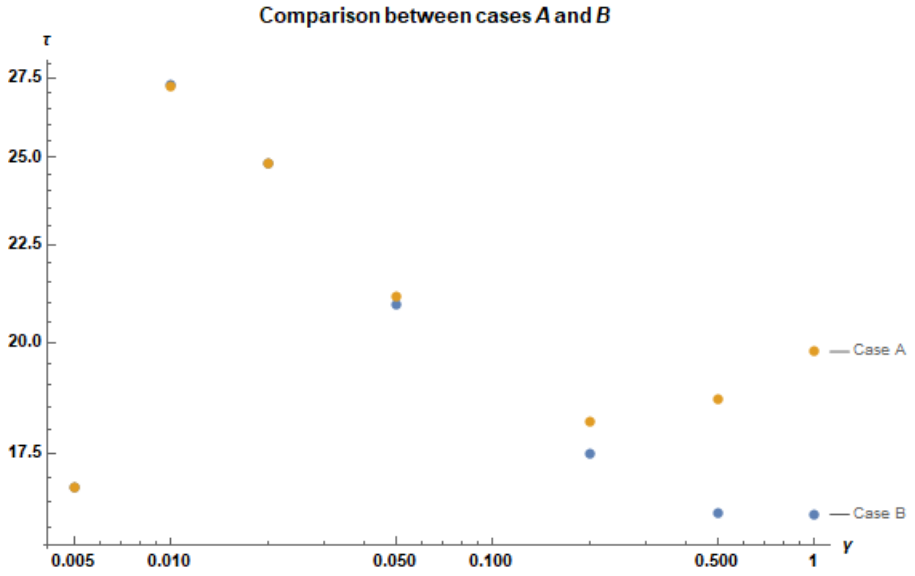

Figure 3.10: Comparison of the logarithmic plots of $\tau_\gamma(\gamma)$, expressed in milliseconds, in the two cases.

In Tables 3.1 and 3.2 we display the values we have obtained for τ_γ relatively to γ, for both the covered cases. In addition, we can visualise the differences in the decorrelation times by comparing the two logarithmic plots of the decorrelation time seen as a function of the connectivity index in figure 3.10: similarly to what we have already observed, the difference between the two situations becomes clearer, if considered in terms of τ_γ, for bigger values of the connectivity index: specifically, in *case B* τ_γ keeps decreasing as γ grows towards one, while in *case A* it starts increasing after $\gamma = 0.2$.

$\boldsymbol{\gamma}$	0.005	0.01	0.02	0.05	0.2	0.5	1
$\boldsymbol{\tau_\gamma}$ (ms)	16.8	27.2	24.8	21.1	18.2	18.7	19.8

Table 3.1: Table of decorrelation times τ_γ relative to each of the values of γ taken into account, when neurons can only be connected once (*case A*).

$\boldsymbol{\gamma}$	0.005	0.01	0.02	0.05	0.2	0.5	1
$\boldsymbol{\tau_\gamma}$ (ms)	16.8	27.3	24.8	20.9	17.5	16.3	16.3

Table 3.2: Table of decorrelation times τ_γ relative to each of the values of γ taken into account, when neurons can establish more than one connection with each other (*case B*).

Conclusions

The study of the brain, and in particular of the networks of neurons that are part of it, is of relevant interest because of the many implications that a better understanding of such a complex machine could have: it could shed further light on how we learn, remember, adapt to change and to physiological traumas, also allowing us to better comprehend and, thus, medically treat issues related to damaged or improperly functioning neural circuits. In addition, getting to know the brain and neural networks more in detail could let us improve the actual models used in order to artificially reproduce and exploit their main strengths, such as their high flexibility and their very efficient parallelisation, be it for faster and more complex calculations or for the realisation of smarter AI.

Experimental evidence suggests that, in order to study more in depth the brain's information processing and computations performing, correlations between neurons are to be taken into account. Indeed, the recent introduction of new techniques such as multielectrode arrays has encouraged the measure of various types of correlations in their temporal and spatial dependence, hence leading to an increment of data about their properties and the information they provide about the way the brain works.

In the present work we have considered a neural network of 1000 half excitatory and half inhibitory neurons described in terms of the *stochastic rate model*, whereby neural units can undergo a change in their state from active to quiescent and vice versa in a probabilistic way. We have investigated, by simulating our network's time-evolution for $50\ ms$, the time-dependence of the autocorrelation coefficient ρ for the total number of spiking nerve cells, in the hypothesis of wide-sense stationarity for its time-evolution process. Specifically, we have carried out our work by analysing the aforesaid autocorrelation coefficient in dependence of the number of outwards connections each neuron had, which we expressed through the introduction of the parameter γ. This parameter has been given two different connotations: in a first case, referred to *case A*, we have considered a network where each neuron could be connected only once to another neuron, thus letting γ convey directly information about the percentage of other units each neuron was connected to. Secondly, in *case B*, we have loosened our restrictions by giving neurons the chance to form more than one connection with the same unit, in which case γ only carried information about the number of outwards branching connections each nerve

cell had. Moreover, we have chosen to deal, for both excitatory and inhibitory synaptic transmissions, with constant values for the synaptic weights w_{ij}, setting them equal to each other. This has led to a further difference between the two cases which has affected the outcomes of our simulations: the second case, as a matter of fact, differed from the first also in having different connection strengths between different couples of neurons, specifically dependent on the number of connections each neuron had formed with that specific unit.
By exploring the time-evolution of ρ for different values of γ, we have observed that it decreased monotonously towards zero and, although it showed a dependence from the value of γ, it did not appear to follow a specific γ-related trend.
We have subsequently compared $\rho's$ time-evolution in the two cases, for each γ-value considered, and we have noticed that the difference in the time-evolution of the autocorrelation coefficient became clearer for bigger values of γ, specifically starting from 0.2, which suggested that the divergence in the effective meaning of γ between the two cases, together with the different connections distributions, played a relevant role. Specifically, the comparisons always resulted in the aforementioned *case B* presenting a $\rho(t)$ decreasing faster and getting closer to 0: since the different effective value of γ had not proven itself responsible for this common trend in the first observations, it had to be ascribed to the different and stronger synaptic connections available in the second case. In addition, by calculating and comparing what we referred to as *decorrelation time* τ_γ in dependence of γ, we have once again noticed the same diverging trend between the two cases for big values of γ.
Further study about the role of connectivity for a stochastic model of neural networks could be implemented by considering non-constant values for the synaptic strengths, letting connections, either only excitatory or both excitatory and inhibitory, to be established only once with one specific unit and be modified according to plasticity rules as in phenomenological spike-time dependent plasticity models. This could incorporate aspects of both the cases we have studied. Moreover, another possible choice could be to vary some of the parameters that could take part, considered in relation to γ, in ρ's time-evolution, such as the total number of neurons and the ratio between excitatory and inhibitory populations; in addition, spatial dependence could be introduced in the study by taking a spatial structure into account and letting connections to be formed only between relatively close neurons, in dependence of the network's connectivity.

Appendix

The inversion generating method

The inversion generating method, also known as *inverse transform sampling* and *inverse transformation method*, is a method based on the Monte Carlo techniques that allows to generate random numbers distributed according to any selected probability distribution, be it continuous or discrete, using (pseudo)random numbers extracted according to a uniform distribution.
If we are interested in generating real numbers x following the probability density function $f(x)$, we first consider the related distribution function $F(x)$, defined as

$$F(x) = \int_{-\infty}^{x} f(x')\, dx',$$

such that $F(x_0)$ represents the probability that x is lower than or equal to x_0. From the nature of $f(x)$ and the normalisation condition, we have that $F(x)$ is a non-decreasing function of x and

$$\lim_{x \to -\infty} F(x) = 0,$$
$$\lim_{x \to +\infty} F(x) = 1.$$

In case the random variable is discrete, $F(x)$ is a non-decreasing step function. Of course, if x belongs to an interval $[a, b]$ instead of $(-\infty, +\infty)$ over which $f(x)$ is normalised, the same results hold if we substitute a and b for $-\infty$ and $+\infty$ respectively.

The inverse generating method consists in first drawing a random number u from the uniform distribution on $[0, 1]$, and then taking for the sought x the value that satisfies the equation $F(x) = u$, ergo

$$x = F^{-1}(u),$$

where the existence of $F^{-1}(u)$ is ensured because of the properties of $F(x)$ we have mentioned above.
In order to prove this, let's consider the probability that a number x_0 generated according to the previous formula will lie between x and $x + dx$: this probability is the same as the probability that u above will lie between $F(x)$ and $F(x + dx)$, which is equal to their difference because of the nature

of u's original probability distribution. Therefore, as a consequence of the very definition of $F(x)$ and the fundamental theorem of calculus, we have

$$F(x + dx) - F(x) = f(x)dx,$$

thus proving the validity of our initial hypothesis.
In Chapter 2 we are interested in using this method for the generation of a number x according to the probability density function

$$f(x) = \alpha e^{-\alpha x},$$

where $0 \leq x < \infty$ and α is a positive constant number. Hence, since

$$F(x) = \alpha \int_0^x e^{-\alpha x'} \, dx' = 1 - e^{-\alpha x},$$

it is easy to see that inverting $F(x) = u$ leads to

$$x = \frac{1}{\alpha} \ln\left(\frac{1}{u}\right) = -\frac{1}{\alpha} \ln(u).$$

In the discrete case, if we wish to generate an integer i according to the probability mass function $p(i)$ and define

$$F(i) = \sum_{j=-\infty}^{i} p(j),$$

the inversion generating method tells us to draw a random number r uniformly on the unit interval and to look for the i such that

$$F(i-1) < r \leq F(i).$$

Bibliography

[1] Arbib, M.A., *The Handbook of Brain Theory and Neural Networks*, The MIT Press, 2002.
[2] Kandel, E., Schwartz, J., Jessell, T., *Principles of Neural Science*, McGraw-Hill Medical, 2000.
[3] Dayan, P., Abbot, L.F., *Theoretical Neuroscience*, The MIT Press, 2001.
[4] Hertz, J., Krogh, A., Palmer, R.G., *Introduction to the Theory of Neural Computation*, Westview Press, 1991.
[5] Gerstner, W., Kistler, W.M., *Spiking Neuron Models. Single Neurons, Populations, Plasticity*, Cambridge University Press, 2002.
[6] Freeman, J.A., Skapura, D.M., *Neural Networks. Algorithms, Applications and Programming Techniques*, Addison-Wesley Publishing Company, 1991.
[7] McCulloch, W.S., Pitts, W. (1943), *A logical calculus of the ideas immanent in nervous activity*. Bulletin of Mathematical Biophysics 5, 115-133.
[8] Hopfield, J.J. , *Neural Networks and Physical Systems with Emergent Collective Computational Abilities*. Proceedings of the National Academy of Sciences, USA 79, 2554 2558. 1992.
[9] Cowan, J.D. (1968), *Statistical mechanics of nervous nets*, Caianiello ER, ed. Neural Networks, Springer, Berlin-Heidelberg-New York, 181-188.
[10] Benayoun, M., Cowan, J.D., van Drongelen, W., Wallace, E. (2010), *Avalanches in a Stochastic Model of Spiking Neurons*. PLoS Comput Biol 6(7): e1000846.
[11] van Kampen, N.G., *Stochastic Processes in Physics and Chemistry*, North-Holland Personal Library, 2007.
[12] Gillespie, D.T. (1976), *A general method for numerically simulating the stochastic time evolution of coupled chemical reactions*, Journal of Computational Physics 22, 403-434.
[13] Gillespie, D.T. (1977), *Exact stochastic simulation of coupled chemical reactions*, The Journal of Physical Chemistry 81 (25), 2340-2361.
[14] Park, K.I., *Fundamentals of Probability and Stochastic Processes with Applications to Communications*, Springer, 2018.
[15] Abeles, M., *Corticonics: Neural Circuits of the Cerebral Cortex*, Cambridge University Press, 1991.
[16] Beggs, J., Plenz, D. (2003), *Neuronal Avalanches in Neocortical Circuits*, Journal of Neuroscience 23: 11167.

[17] Cohen, M. R., Kohn, A. (2011), *Measuring and interpreting neuronal correlations*, Nature Neuroscience 14, 811-819.
[18] Greschner, M. et al. (2011), *Correlated firing among major ganglion cell types in primate retina*, J. Physiol. (Lond.) 589, 75-86.
[19] Alonso, J.M., Martinez, L.M. (1998), *Functional connectivity between simple cells and complex cells in cat striate cortex*, Nat. Neurosci. 1, 395-403.
[20] Gillespie, D.T., *The Monte Carlo method of evaluating integrals*, Naval Weapons Center China Lake, California, 1975.
[21] Amit, D.J., Gutfreund, H., Sompolinsky, H. (1985), *Spin-glass models of neural networks*, Physical Review A 32, 1007-1018.
[22] Erto, P., *Probabilità e statistica per le scienze e l'ingegneria*, McGraw-Hill, 2008.
[23] Colucci D'Amato, L., di Porzio, U., *Introduzione alla neurobiologia. Meccanismi di sviluppo, funzione e malattia del sistema nervoso centrale*, Springer-Verlag Italia, 2011.
[24] Hebb, D.O., *The Organization of Behavior: A neuropsychological theory*, Wiley, 1949.
[25] Zhang, L.I., Tao, H.W., Holt, C.E., Harris, W.A., and Poo, M.M. (1998), *A critical window for cooperation and competition among developing retinotectal synapses*, Nature, 395:37-44.
[26] Bi, G.Q., Poo, M.M. (1998), *Synaptic modifications in cultured Hippocampal neurons: dependence on spike timing, synaptic strength, and postsynaptic cell type*. J Neurosci, 18:10464-72.
[27] Markram, H., Lübke, J., Frotscher, M., Sakmann, B. (1997), *Regulation of synaptic efficacy by coincidence of postsynaptic APs and EPSPs*. Science, 275:213-215.